Mon. Not. R. Astron. Soc. **000**, 1–6 (2010) Printed 17 February 2019 (MN LATEX style file v2.2)

Willman 1 in X-rays: Can you tell a dwarf galaxy from a globular cluster?

N. Mirabal[1,2⋆] and D. Nieto[2]
[1] *Ramón y Cajal Fellow*
[2] *Dpto. de Física Atómica, Molecular y Nuclear, Universidad Complutense de Madrid, Spain*

ABSTRACT
We present an analysis of a deep archival *Chandra* observation of Willman 1, an object suspected to straddle the line of what constitutes a dwarf galaxy and an extreme globular cluster. Our main goal is to examine potential observational signatures in X-rays that might distinguish its true identity either through an unusual point source population or based on the existence of prominent diffuse emission in its core. We identify a total of 26 sources within the central $5'$ to a limiting 0.5–2.0 keV X-ray flux of 6×10^{-16} erg cm^{-2} s^{-1}. While some of these sources could be formal members of Willman 1, we find no outstanding evidence for either an unusual population of bright X-ray sources or a densely populated cluster core. In fact, the entire X-ray population could be explained by background active galactic nuclei and/or foreground stars unrelated to Willman 1. As a result, there is no substantial evidence in X-rays to argue against a dwarf galaxy classification for Willman 1 down to current observational limits. This result enhances the qualifications of Willman 1 as an ideal target for indirect dark matter searches. Accordingly, we derive upper limits for a possible sterile neutrino signature with a mass of 1.6–16.0 keV and finish with a discussion of previous measurements.

Key words: X-rays: general – globular clusters: general – galaxies: Local Group, dark matter – galaxies: individual (Willman 1)

1 INTRODUCTION

Defining the divide between ultra-faint dwarf galaxies and extreme globular clusters is one the pressing issues in galaxy formation and evolution. Traditionally, the distinction has relied on metallicity studies and the size-luminosity relation (Willman et al. 2005; Martin et al. 2007). In general, globular clusters tend to be more compact than dwarf galaxies and appear to be dominated by a single-metallicity population. However, the recent discovery of ultra-faint objects with few identified stars has blurred some of these distinctions (Willman et al. 2005; Siegel, Shetrone & Irwin 2008; Niederste-Ostholt et al. 2009).

At the most fundamental level, the fraction of dark matter that remains in the central region of such systems could be at the heart of the division (Baumgardt & Mieske 2008). Observationally, however, the distinction appears to be more complicated. A clean separation of dwarf galaxies and stellar clusters is critical for a number of reasons. Chief among them is the need to obtain a reliable count of the number of dwarf galaxies present in the Local Group. Cold dark matter (CDM) simulations estimate that hundreds of dwarf galaxies should be present in the Local Group (Blumenthal et al. 1984; Davis et al. 1985). However, despite the best efforts to date, it has been noted that the number of dwarf galaxies produced in cosmological simulations is at least a factor of magnitude higher than the actual number of dwarf galaxies observed around the Milky Way (Klypin et al. 1999; Moore et al. 1999). Fortunately, the advent of novel imaging techniques and deeper wide-field optical/IR surveys are helping complete the census of satellites in the Local Group (Mateo 1998; Willman et al. 2005; Belokurov et al. 2007). Thus, a detailed criterion that separates dwarf galaxies from extreme globular clusters will be necessary to establish the divergence between actual observations and cosmological simulations.

Another motivation for a clear classification scheme is the need to further evaluate the credentials of ultra-faint objects as targets for indirect dark matter searches. Dwarf galaxies are expected to be dark matter dominated, making them excellent targets to conduct searches for the annihilation and decay of dark matter particles at high energies (Strigari et al. 2008). This contrasts with results from numerical simulations showing that dark matter gets removed

⋆ E-mail: mirabal@gae.ucm.es

from the central regions of globular clusters due to dynamical friction (Baumgardt & Mieske 2008). Confirmation of such prediction would render globular clusters less interesting than dwarf galaxies for indirect dark matter searches.

In this paper we investigate whether X-ray observations might help distinguish dwarf galaxies from globular clusters. The superb resolution of *Chandra* and *XMM-Newton* has revealed a complex population of binary systems in globular clusters (Grindlay et al. 2001; Heinke et al. 2003; Servillat, Webb & Barret 2008). Theoretical predictions conclude that cataclysmic variables (CVs) and low mass X-ray binaries (LMXBs) should be formed quite efficiently in globular clusters due to frequent dynamical interactions (Clark 1975; Fabian, Pringle & Rees 1975; Pooley & Hut 2006). Indeed, X-ray observations confirm that globular clusters are 100 times more likely to host LMXBs than galactic fields (Irwin 2005; Kundu, Maccarone & Zepf 2007).

In contrast, the formation of close binaries should be more challenging in the field populations of dwarf galaxies (Maccarone et al. 2005; Ramsay & Wu 2006). As a result, a complete study of the population of X-ray sources in the core of a globular cluster should make it stand out over a dwarf galaxy observed to the same depth. Here, rather than trying to prove a dwarf galaxy identity, we seek to exclude or favor a globular cluster X-ray classification for objects in dispute.

We explore such possibility using a deep archival *Chandra* observation of the enigmatic Galactic satellite Willman 1 (Willman et al. 2005). Willman 1 is an ultra-faint object discovered in the Sloan Digital Sky Survey (SDSS) and initially classified as a dwarf galaxy (Willman et al. 2005, 2006). However, further studies cast some doubts around the true identity of this object (Siegel, Shetrone & Irwin 2008). The alternative is that Willman 1 is in fact a tidally disrupted globular cluster that impersonates a dwarf galaxy. Here, we explore these possibilities in X-rays. The organization of the paper is as follows. §2 describes the X-ray observations. Source identification and spectral analyses are discussed in §3. In §4 we measure the diffuse component of Willman 1 and examine the parameter space for sterile neutrinos allowed by the data. Summary and conclusions are presented in §5.

2 OBSERVATIONS

Willman 1 was observed by the *Chandra X-ray Observatory* for 102.75 ks on 2009 January 27–28 (*Chandra* ObsID 10534) as described in Loewenstein & Kusenko (2009). Observations were conducted with the Advanced CCD Imaging Spectrometer (ACIS) in very faint (*VFAINT*) mode. Chips 0,1,2,3,6,7 were used with Willman 1 positioned near the ACIS-I aimpoint on the ACIS-I3 chip. Data reduction was performed using standard procedures [1] within the *Chandra* Interactive Analysis of Observations (CIAO) software. The level 1 event file was reprocessed to include grades 0,2,3,4, and 6. The total usable data is reduced to 100.68 ks after removing periods of potential flares and elevated background. Figure 1 shows the resulting *Chandra* X-ray (0.5–6.0 keV) image. The X-ray image has been smoothed with a Gaussian kernel with radius $r_k = 2.5''$.

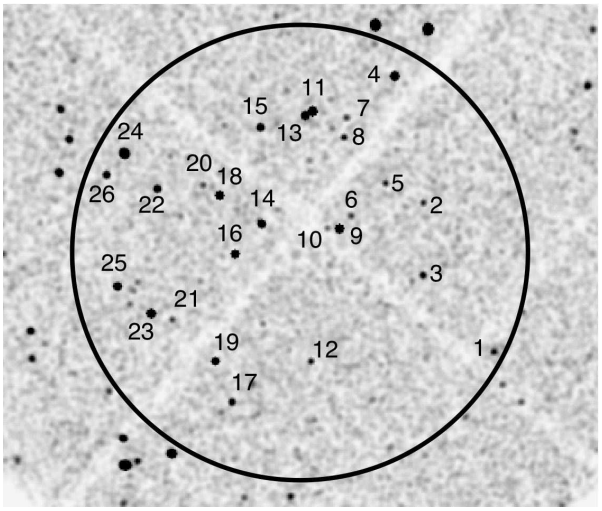

Figure 1. *Chandra* ACIS-I image of Willman 1 in the 0.5–6.0 keV energy range. The X-ray image has been smoothed with a Gaussian kernel with radius $r_k = 2.5''$. Identified sources are marked following the labels adopted in Table 1. The circle is centered on RA. $10^{\rm h}49^{\rm m}22\overset{\rm s}{.}3$, Dec. $+51°03'03''$ and drawn with a $5'$ radius. The half-light radius corresponds to $r_{1/2} = 1.9'$. Notice that the placement falls near the intersection of the chip gaps.

We searched for point sources within the central $5'$ of Willman 1 using the CIAO tool *celldetect*. This corresponds to a physical size of 55 pc assuming a distance of 38 kpc. This region encompasses the half-light radius of Willman 1 estimated to be $r_{1/2} = 1.9'$ (Willman et al. 2006). Figure 1 shows all 26 detections with more than 15 net counts in the 0.5–6.0 keV energy range. Ten of the sources are on the I1 chip, seven on the I2 chip, six on the I0 chip, and three on the I3 chip.

X-ray counts were extracted within a $2.5''$radius circles centered on the source location. The counts were then separated in three different energy ranges: a *soft* band (0.5–1.5 keV), a *medium* band (0.5-4.5 keV), and a *hard* band (1.5-6.0 keV). Finally, we estimated net counts using source-free background regions in the corresponding individual chip. The source labels, positions, and net counts in three separate energy bands are listed in Table 1.

3 SOURCE IDENTIFICATION AND SPECTRAL ANALYSIS

The principal obstacle in sorting out whether any individual point source in the field represents a *bona fide* member of Willman 1 is the inescapable presence of background active galactic nuclei (AGN) in the field (Giacconi et al. 2001; Luo et al. 2008). It turns out to be extremely difficult to distinguish the source identity whenever the number of predicted background AGN matches the observed number of sources in the field (Ramsay & Wu 2006). In this instance, a detection limit of 15 net counts in the 0.5–6 keV energy range corresponds to a limiting flux 6×10^{-16} erg cm^{-2} s^{-1} in the 0.5–2.0 keV band, adopting an X-ray power spectral index $\Gamma = 1.4$ and a Galactic H I column density $N_{\rm H}$

[1] http://cxc.harvard.edu/ciao/threads/aciscleanvf/

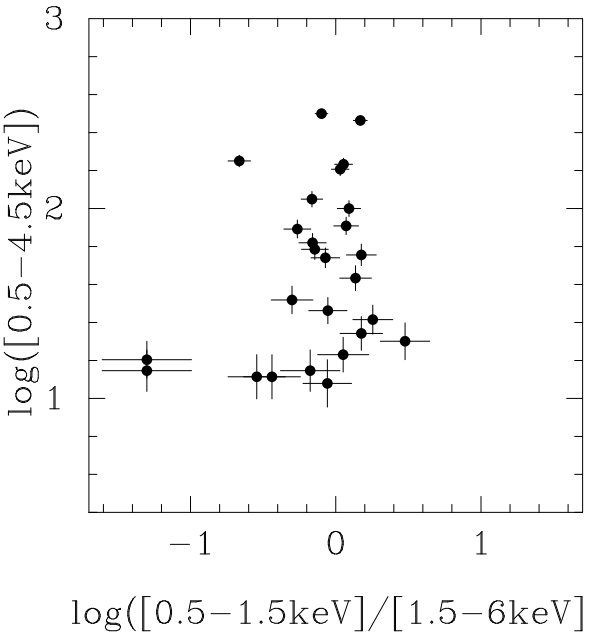

Figure 2. X-ray colour-magnitude diagram for 26 sources detected within the inner 5′ of Willman 1.

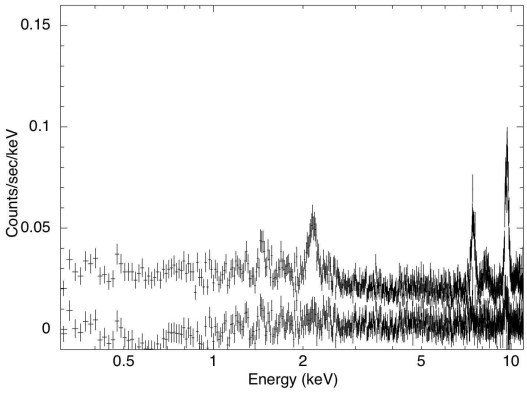

Figure 3. *Chandra* ACIS-I spectrum extracted from a 5′ radius circle centered on Willman 1 as described in the text.. *Top:* Data prior to removal of the background. Instrumental line features include Si K α (1.74 keV), Au M α, β (2.1–2.2 keV), Ni K α (7.47 keV), and Au L α (9.67 keV). *Bottom:* Spectrum after background subtraction.

$= 1.2 \times 10^{20}$ cm^{-2}. Using the latest AGN counts from the *Chandra* Deep Field-South (CDFS) reported by Luo et al. (2008), we expect an average of 24±3 background AGN for a field of this size to our limiting flux in the 0.5–2.0 keV band. Our detection of 26 sources does not exceed significantly the CDFS prediction. As a result, the majority of sources found are most likely background AGN.

In order to test this prediction, we proceeded to evaluate the variability and colour of the individual sources. The presence of binary systems might be exposed through the detection of strong variability (Heinke et al. 2003). According to the CIAO tool *glvary*, there are no definite variables among the point sources. Similarly, the location of a source in an X-ray colour magnitude diagram (CMD) might be a powerful way to infer the presence of binary systems in a field (Grindlay et al. 2001). In particular, certain CVs/LMXBs will depart from AGN and become outliers in the colour distribution. In Figure 2 we plot the logarithm of the 0.5–4.5 keV counts versus the logarithm of the ratio of 0.5–1.5 keV and 1.5–6.0 keV net counts. Note that the majority of the sources tend to gather around the center of the diagram where it is difficult to tell binary systems and AGN apart. However, the void in the upper right corner of the diagram probably rules out the presence of LMXBs in quiescence (Heinke et al. 2003). The two hard sources to the left of the diagram could indicate heavily obscured AGN but the reduced number of counts prevents a formal identification. Therefore, the colour analysis fails to discover any apparent binary system in the field.

Additional clues might be gained from the examination of the actual spectra of the sources. For this reason, spectra were generated for all the sources with 50 or more detected counts in the 0.5–6.0 keV energy band. This criterion leaves 13 out of the total sample of 26 sources. The counts for each source were grouped using the CIAO tool *dmgroup* such that there are 10 counts per bin. By default, we adopted a power-law model spectral fit within XSPEC (Arnaud 1996) with the absorption fixed at the Galactic value $N_{\rm H} = 1.2 \times 10^{20}$ cm^{-2}. Power law fits with indices $1.2 < \Gamma < 2$ are acceptable ($\chi^2_\nu < 1.5$) to all sources, except source 14. For the latter a blackbody or models with substantial internal absorption provide better fits. However, it is difficult to make a final spectral classification for that source. Overall, the spectral results are consistent with the properties of background AGN in such a field. We note that there is also a non-negligible probability that a handful of coronal emitting stars in the foreground could be superposed by chance along the line of sight (Haggard, Cool & Davies 2009). As a consequence, there is no reason to conclude that the point source population in the field is associated with Willman 1.

4 DIFFUSE EMISSION AND THE SEARCH FOR A DARK MATTER SIGNATURE

Having found no disarming argument against a dwarf galaxy classification among the point source population, we turn our attention to the diffuse emission in and around Willman 1. Based on the high mass-to-light ratio (~ 700) inferred by Martin et al. (2007), Willman 1 has emerged as an attractive target for indirect dark matter searches (Strigari et al. 2008). Yet, to date no dark matter signal has been observed in sensitive observations of Willman 1 at energies > 100 MeV (Aliu et al. 2009; Abdo et al. 2010).

In X-rays, one expect that the diffuse emission in Willman 1 will be dominated either by an unresolved point source population or by a complex gaseous component (Hui, Cheng & Taam 2009). However, there is also a possibility that the dark matter halo of Willman 1 might produce a detectable X-ray flux made primarily of hypothesized warm dark matter (WDM) particle decays into photons in the 0.3–10 keV energy range (Abazajian, Fuller & Tucker 2001; Boyarsky et al. 2006; Loewenstein, Kusenko & Biermann 2009).

One natural WDM particle candidate is the sterile neutrino, a weakly-interacting fermion associated with the neutrino sector that arises in some extensions of the standard model (Dodelson & Widrow 1994). The principal decay channel for sterile neutrinos is into three light active neutrinos. There is a potentially detectable radiative decay channel in the X-ray band, whereby a lighter active neutrino and a X-ray photon are produced with a slow mean decay on the order of the lifetime of the Universe (Abazajian, Fuller & Tucker 2001). The former is a two-body decay, meaning that the resulting photon energy distribution is characterized by a spectral line with a broadening due to the velocity dispersion of the original sterile neutrinos. Interestingly, such neutrinos may mitigate some of the shortcomings of cold dark matter cosmologies including the apparent dearth of dwarf galaxies around the Milky Way (but see de Naray et al. 2010).

In order to survey the diffuse emission, we excised all point sources within the inner $5'$ of Willman 1. Due to an unfortunate placement of the object within the ACIS footprint, the diffuse emission is missing a critical section of the inner core of Willman 1 and extends over four distinct ACIS-I CCDs with distinct gains (see Figure 1). In order to avoid significant intrachip variations, we excluded 32 pixels to each side of the CCD edges. Visual examination of the resulting X-ray image does not reveal prominent diffuse emission that would give away a rich globular cluster core. Given the intrachip gain fluctuations across the CCDs, it is not straightforward to ascertain the significance of the counts within the inner $5'$ of Willman 1. We note however that the limited signal-to-noise ratio and placement across four CCDs cannot ensure that the detected counts correspond to diffuse emission specific to Willman 1. Rather the counts might result from Poisson fluctuations in the background count rate.

On the other hand, it is possible to derive upper limits on the diffuse emission after subtracting the background contribution at this position. The spectrum of the diffuse emission was rendered from a $5'$ radius circle at the nominal position of Willman 1 of RA. $10^{\rm h}49^{\rm m}22\overset{\rm s}{.}3$, Dec. $+51°03'03''$ and corrected with the standard reprojected blank-sky background (Markevitch et al. 2003). The final step consisted in a renormalization of the background spectrum to match the 9.0–12.0 keV count rate of the Willman 1 exposure. Figure 3 shows the spectrum before and after subtraction of the background. Prior to subtraction, the spectrum is dominated by prominent instrumental line features that originate from fluorescence of material in the telescope including Si K α (1.74 keV), Au M α, β (2.1–2.2 keV), Ni K α (7.47 keV), and Au L α (9.67 keV). The instrumental features are largely removed after subtracting the background.

In order to establish upper limits to the emission of dark matter in the energy range covered by the observation, we fit the spectrum in steps of 0.1 keV with the appropriate Gaussian width σ required to match the spectral resolution at each step. This emulates the procedure outlined in previous analyses of *Chandra* data (Mirabal, Paerels & Halpern 2003; Riemer-Sørensen, Hansen & Pedersen 2006). We next proceeded to derive limits coming from a dark matter halo composed of sterile neutrino particles with rest mass 1.6 keV $< m_\nu <$ 16.0 keV as a function of mixing angle θ following the derivation described in Loewenstein & Kusenko (2009).

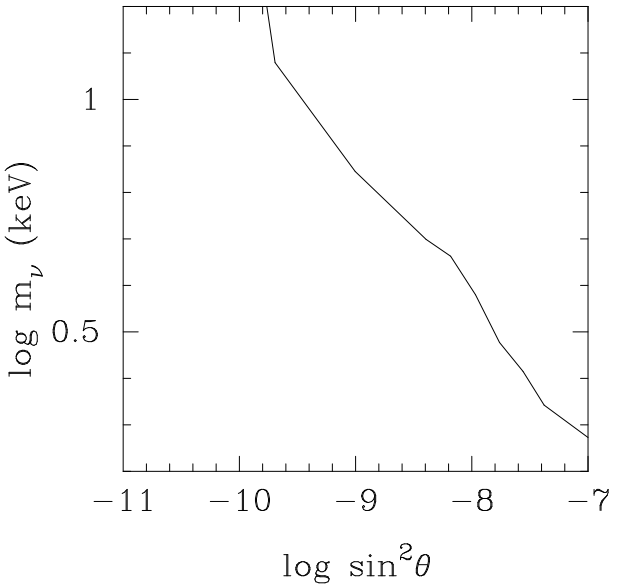

Figure 4. Parameter space constraints for the sterile neutrino. The region to the right of the contour is ruled out by the *Chandra* observation of Willman 1.

Figure 4 shows the resulting sterile neutrino parameter space ruled out by the *Chandra* observation. This limit assumes that the dark matter halo is composed exclusively of sterile neutrinos. Except for some minor differences, our results for the parameter space are consistent with the results originally reported by Loewenstein & Kusenko (2009).

However, we differ from Loewenstein & Kusenko (2009) in that we find no evidence for a purported line detection at 2.51 keV with a line flux $f_{line} = 3.53 \times 10^{-6}$ photons cm^{-2} s^{-1}. Figure 5 shows the background-subtracted ACIS spectrum in the 2.0–5.0 keV energy region. An absorbed power-law model fixed at the Galactic H I column density $N_{\rm H} = 1.2 \times 10^{20}$ cm^{-2} and photon index $\Gamma = 1.0 \pm 0.6$ appears to accommodate the data ($\chi^2_\nu = 0.86$). There is an excess around 2.3–2.5 keV, but the inclusion of a Gaussian line with the properties reported in Loewenstein & Kusenko (2009) does not improve the fit ($\chi^2_\nu = 0.85$). Leaving the power-law index to be a free parameter and allowing the Gaussian line centroid wander in the 2.0–3.0 keV energy yields an unrealistic $\Gamma = -1.2 \pm 0.7$ with a Gaussian line centered at 2.2 keV. The latter is most likely due to the instrumental Au M α, β (2.1–2.2 keV) line and highlights the difficulties with reported line detections in and around this region. Thus, while we cannot rule out weak emission between 2.3 and 2.5 keV, we find that a power-law model provides a satisfactory fit without the need for the Gaussian line reported by Loewenstein & Kusenko (2009).

Upon closer inspection of Figure 1 in Loewenstein & Kusenko (2009) we notice spectral residuals in the vicinity of the aforementioned instrumental lines of Au M α, β (2.1–2.2 keV), Ni K α (7.47 keV), and Au L α (9.67 keV). We face similar issues in our analysis that seem entirely consistent with a diffuse emission signal heavily dominated by background spectrum (see also Boyarsky et al. 2010). In such circumstances, it is possible that a deficient subtraction of the Au M α, β (2.1–2.2 keV) instrumental line or calibration issues at

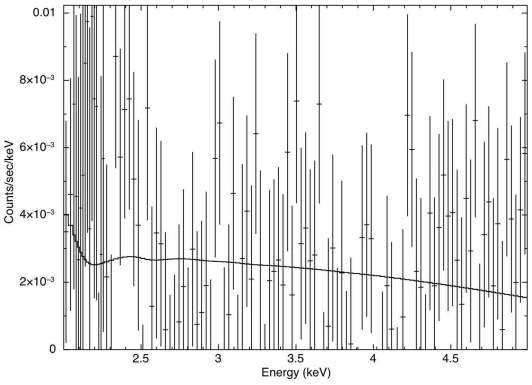

Figure 5. *Chandra* ACIS spectrum of the diffuse component of Willman 1 in the 2.0-5.0 keV energy range and best-fitting absorbed power-law model as described in the text.

$E < 2.3$ keV will start to carve the silhouette of a spectral line around 2.4–2.5 keV that might result in the finding reported in Loewenstein & Kusenko (2009). In addition, it is difficult to discard that intrachip gain variations may conspire to mimic an emission line. It is important to recall that spurious X-ray line detections have a curious history in the literature (Sako, Harrison & Rutledge 2005; Vaughan & Uttley 2008). Henceforth, one must be careful when dealing with marginal detections (Protassov et al. 2002).

Even if one wants to advocate the reality of a line at 2.51 keV, a direct dark matter connection suffers from a fatal flaw in that it falls at a location matching the rest-frame of helium-like sulphur ion S XV α located at 2.45 keV (Raymond & Smith 1977). This astrophysical line is routinely detected in plasmas with temperatures $\sim 10^{6-7}$ K (Hwang et al. 2004; Henley et al. 2008). Consequently, it seems more plausible that one is detecting sulphur emission from a hot supernova remnant or a highly-ionized wind region either at Willman 1 itself or at an intervening location to the object, rather than the exotic signature of dark matter.

5 SUMMARY AND CONCLUSIONS

At this stage, we find no evidence in X-rays to question the classification of Willman 1 as a dwarf galaxy. Adopting an estimated distance of 38 kpc, it might be the case that the bulk of sources connected with Willman 1 lies below our luminosity limit of 10^{32} erg s^{-1} in the 0.5–2.0 keV energy band, as in the case of globular cluster GLIMPSE-C01 (Pooley et al. 2007). Consequently, X-ray observations might only serve to exclude extreme globular clusters with an unusual concentration of bright emitters or eccentric cores. However, combined with optical imaging, X-ray observations will be decisive in purging the sample used for size-luminosity and metallicity studies. Furthermore, X-ray observations will be able to investigate if a significant point-source population capable of mimicking a dark matter signal is present in the field.

Given the existing limits, it might be wise to concentrate on the detectability of the sterile neutrino with future X-ray experiments as it will be difficult to improve current measurements with the existing instrumentation (Abazajian 2009). In particular, making the case for future calorimeter experiments that could definitely detect it or exclude it as a dark matter candidate (F. Paerels, private communication). We have shown here that any viable indirect search for dark matter in this energy range must deal not only with possible overlap with instrumental lines in the spectrum (Riemer-Sørensen, Hansen & Pedersen 2006), but also with possible contamination from intervening plasma lines that may mask a dark matter origin. We caution that extraordinary claims related to dark matter should be backed by outstanding observational evidence (Sagan 1980).

With the Large Hadron Collider (LHC) and other laboratory experiments coming online, it might be possible to achieve a direct detection of the particles responsible for dark matter. However, any direct detection in the laboratory will then have to be followed by confirmation or dismissal of sameness in an astrophysical context. Based on the present study, Willman 1 continues to hold a select place among targets to conduct such searches. It is worth noting that within the inner $5'$ radius circle of Willman 1, there are no radio sources at 1.4 GHz in the NRAO VLA Sky Survey (NVSS) source catalog (Condon et al. 1998). Moreover, we have shown that the point source population to a limiting 0.5–2.0 keV X-ray flux of 6×10^{-16} erg cm^{-2} s^{-1} is consistent with background AGN and/or foreground stars. The available data from radio through X-rays thus make Willman 1 a notable candidate for the eventual astrophysical verification of a dark matter particle.

ACKNOWLEDGMENTS

N.M. acknowledges support from the Spanish Ministry of Science and Innovation through a Ramón y Cajal fellowship. We thank all the members of Grupo de Altas Energías (GAE) at the Universidad Complutense de Madrid for stimulating discussions. We also acknowledge support from the Consolider-Ingenio 2010 Programme under grant MULTIDARK CSD2009-00064.

REFERENCES

Abdo A. A., Ackermann M., Ajello M. et al., 2010, ApJ, accepted (arXiv:1001.4531)
Aliu E., Anderhub H., Antonelli L. A. et al., 2009, ApJ, 697, 1299
Arnaud K. A., 1996, in Jacoby G. H., Barnes J., eds, Astronomical Data Analysis Software and Systems V. Astron. Soc. Pac., San Francisco, p. 17
Abazajian K., Fuller G. M., Tucker W. H., 2001, ApJ, 562, 593
Abazajian K. N., 2009, preprint (arXiv:0903.2040)
Baumgardt H., Mieske S., 2008, MNRAS, 391, 942
Belokurov V., Zucker D. B., Evans N. W. et al., 2007, APJ, 654, 897
Blumenthal G. R., Faber S. M., Primack J. R., Rees M. J., 1984, Nature, 311, 517

Boyarsky A., Neronov A., Ruchayskiy O., Shaposhnikov M., 2006, MNRAS, 370, 213
Boyarsky A., Ruchayskiy O., Iakubovskyi D. et al., 2010, preprint (arXiv:1001.0644v1)
Clark G. W., 1975, ApJ, 199, L143
Condon J. J., Cotton W. D., Greisen E. W., Yin Q. F., Perley R. A., Taylor G. B., Broderick J. J., 1998, AJ, 115, 1693
Davis M., Efstathiou G., Frenk C. S., White S. D., 1985, ApJ, 292, 371
de Naray R. K., Martinez G. D., Bullock J., Kaplinghat M., 2010, ApJ, 710, L161
Dodelson S, Widrow L. M., 1994, Phys. Rev. Lett., 72, 17
Fabian A. C., Pringle J. E., Rees M. J., 1975, MNRAS, 172, 15P
Giacconi R., Rosati P., Tozzi P. et al., 2001, ApJ, 551,624
Grindlay J. E., Heinke C. O., Edmonds P. D., Murray S. S., 2001, Science, 292, 2290
Haggard D., Cool A. M., & Davies M. B., 2009, ApJ, 697, 224
Heinke C. O., Grindlay J. E., Edmonds P. D., LLoyd D. A., Murray S. S., Cohn H. N., Lugger P. M., 2003, ApJ, 598, 516
Henley D. B., Corcoran M. F., Pittard J. M., Stevens I. R., Hamaguchi K., Gull T. R., 2008, ApJ, 680, 705
Hui C. Y., Cheng K. S., Taam R. E., 2009, ApJ, 700, 1233
Hwang U., Martin Laming J., Badenes C. et al., 2004, ApJ, 615, L117
Irwin J. A., 2005, ApJ, 631, 511
Klypin A., Kravtsov A. V., Valenzuela O. et al., 1999, ApJ, 522, 82
Kundu A., Maccarone T. J., Zepf S. E., 2007, ApJ, 662, 525
Loewenstein M., Kusenko A., 2009, ApJ, submitted (arXiv:0912.0552)
Loewenstein M., Kusenko A., Biermann P. L., 2009, ApJ, 700, 426
Luo B., Bauer F. E., Brandt W. N. et al., 2008, ApJS, 179, 19
Maccarone T. J., Kundu A., Zepf S. E., 2005, MNRAS, 364, L61
Markevitch M., Bautz M. W., Biller B. et al., 2003, APJ, 583, 70
Martin N. F., Ibata R. A., Chapman S. C., Irwin M., Lewis G. F., 2007, MNRAS, 380, 281
Mateo M. L., 1998, ARA&A, 36, 435
Mirabal N., Paerels F., Halpern J. P., 2003, ApJ, 587, 128
Moore B., Governato F., Lake G. et al., 1999, ApJ, 524, L19
Niederste-Ostholt M., Belokurov V., Evans N. W., Gilmore G., Wyse R. F. G., Norris J. E., 2009, MNRAS, 398, 1771
Pooley D., Hut P., 2006, ApJ, 646, L143
Pooley D., Rappaport S., Levine A., Pfahl E., Schwab J., 2007, ApJ, submitted (arXiv:0708.3365)
Protassov R., van Dyk D. A., Connors A. et al. 2002, ApJ, 571, 545
Ramsay G., Wu K., 2006, A&A, 459, 777
Raymond J. C., Smith B. W., 1977, ApJS, 35, 419
Riemer-Sørensen S., Hansen S. H., Pedersen K., 2006, ApJ, 644, L33
Sagan C., 1980, Cosmos. Random House, New York, NY
Sako M., Harrison F. A., Rutledge R. E., 2005, ApJ, 623, 973
Servillat M., Webb N. A., Barret D., 2008, A&A, 480, 397
Siegel M. H., Shetrone M. D., Irwin M., 2008, AJ, 135, 2084
Strigari L. E., Koushiappas S. M., Bullock J. S., Kaplinghat M., Simon J. D., Geha M., Willman B., 2008, ApJ, 678, 614
Vaughan S., Uttley P., 2008, MNRAS, 390, 421
Willman B., Blanton M. R., West A. et al., 2005, AJ, 129, 2692
Willman B., Masjedi M., Hogg D. W. et al., 2006, ApJ, submitted (arXiv:astro-ph/0603486)

Table 1. X-ray sources identified within the central 5′ of Willman 1

Source Label	R.A. (J2000.0)	Dec. (J2000.0)	Net Counts 0.5 – 1.5 keV	0.5 – 4.5 keV	1.5 – 6.0 keV
1	10 48 55.4	+51 00 53.0	1±1	14±4	20±5
2	10 49 05.1	+51 04 09.6	1±1	16±4	20±5
3	10 49 05.2	+51 02 34.5	15±4	29±5	17±4
4	10 49 09.1	+51 06 57.1	94±10	171±13	83±9
5	10 49 10.3	+51 04 35.8	15±4	20±5	5±2
6	10 49 15.1	+51 03 53.2	6±3	14±4	9±3
7	10 49 15.9	+51 06 02.2	9±3	17±4	8±3
8	10 49 16.2	+51 05 36.6	18±4	26±5	10±3
9	10 49 16.8	+51 03 35.6	89±9	161±13	83±9
10	10 49 18.5	+51 03 37.0	7±3	12±4	8±3
11	10 49 20.6	+51 06 10.6	183±14	291±17	124±11
12	10 49 20.8	+51 00 41.3	15±4	22±5	10±3
13	10 49 21.6	+51 06 05.1	46±7	81±9	39±6
14	10 49 27.7	+51 03 41.5	27±5	66±8	39±6
15	10 49 27.8	+51 05 49.3	28±5	55±7	33±6
16	10 49 31.4	+51 03 02.5	58±8	100±10	47±7
17	10 49 31.8	+50 59 47.0	12±4	33±6	24±5
18	10 49 33.6	+51 04 20.0	48±7	112±11	70±8
19	10 49 34.1	+51 00 41.1	28±5	61±8	39±6
20	10 49 35.9	+51 04 33.2	4±2	13±4	11±3
21	10 49 40.2	+51 01 36.0	4±2	13±4	14±4
22	10 49 42.3	+51 04 28.1	36±6	57±8	24±5
23	10 49 43.1	+51 01 44.1	34±6	178±13	157±13
24	10 49 46.9	+51 05 14.7	154±12	316±18	193±14
25	10 49 47.8	+51 02 19.7	31±6	78±9	57±8
26	10 49 49.4	+51 04 46.8	26±5	43±7	19±4